Prediction of the ultimate load-carrying capacity of wooden notched beams with and without reinforcements using a splitting model

Edouard Sorin, Jean-Luc Coureau, Myriam Chaplain

Prediction of the ultimate load-carrying capacity of wooden notched beams with and without reinforcements using a splitting model

Edouard Sorin[a,*], Jean-Luc Coureau[a,**] and Myriam Chaplain[a]

[a]*Université de Bordeaux, UMR 5295, Institut de Mécanique et d'Ingénierie - Bordeaux (I2M), Dépt. Génie Civil et Environnemental (GCE), Bordeaux F-33000, France*

ARTICLE INFO

Keywords:
notched beams
R-curve
predictive model
reinforcement
wood
splitting

ABSTRACT

The present study proposes a new method to predict the ultimate load bearing capacity of structural notched beams subjected to splitting. Reinforced and unreinforced cases are investigated by using a FE-model for splitting failure. The contribution of mode I and mode II in the crack extension mechanisms is implemented in the numerical model by considering a mixed mode criterion established on the R-curves of wood. The influences of the notch and the reinforcements on the resulting quasi-brittle behaviour is analysed. The FE-prediction are compared to experimental data and the current design rules of the Eurocode 5.

1. Introduction

Notched beams present a stress concentration area which can produce the splitting of wood. This type of failure influences significantly the load-bearing capacity of the elements, which requires some specific design methods. The shape and size of the notch govern the mechanical behaviour of the elements. In order to improve the strength of such structural components and to improve the load transfer in wood perpendicular to the grain, local reinforcements are recommended and requires design rules for engineering. In order to improve the knowledge concerning the failure mechanisms occurring in such elements. It is then necessary to introduce new approaches focusing on the prediction of the load bearing capacity of reinforced and unreinforced notched beams.

Nowadays, several design methods exist to estimate the strength of unreinforced wooden notched beams. Most of them are based on the fracture mechanics, but others refer to empirical studies like the Timber Construction Manual [25] and the DIN 1052 of 1988 [12]. As part of fracture mechanics, approaches can be divided in two ways : one may use the energy release rate (G_i) [18], whereas the other consider the stress intensity factor (SIF, K_i) [21]. The Eurocode 5 design method [16] refers to the works realised by Gustafsson [19] which proposes the equation 1. In this approach, the critical shear force of the beam is predicted by considering the critical energy release rate ($G_{c,I}$) in mode I and the stiffness evolution of the beam (obtained from the beam theory). For the Eurocode 5, some coefficients were introduced according to the strength grades of timber [15, 14, 1], and the failure property (critical energy release rate) was deduced from research led on free defect Spruce (*Picea abies.*) [19]. Finally, this proposal depends on the notch geometry (Figure 1) and the wood quality (solid wood or glulam). This approach has the advantage to be useful for engineers and design offices. Nevertheless, it may introduce some bias for the prediction of strength, since wood is regarded as a pure brittle material and the crack propagation mainly considered in mode I. Moreover the formulation is not well adapted for notches with important height.

$$V_d = \frac{b\alpha h\sqrt{\frac{G_{c,I}}{h}}}{\sqrt{\frac{0.6(\alpha-\alpha^2)}{G_{xy}}} + \beta\sqrt{\frac{6(\frac{1}{\alpha}-\alpha^2)}{E_x}}} \tag{1}$$

With :

- V_d the design value of the shear force

edouard.sorin@u-bordeaux.fr (E. Sorin); jean-luc.coureau@u-bordeaux.fr (J. Coureau)
ORCID(s):

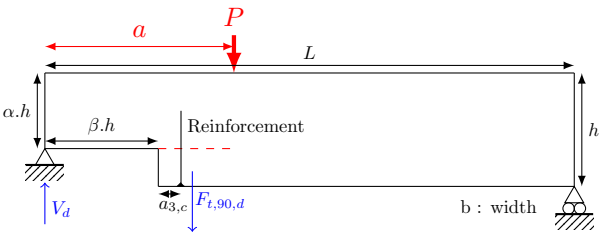

Figure 1: Test protocol diagram with the geometric parameters of the reinforced beams

- G_{xy} the shear modulus
- E_x the longitudinal Young modulus

Some other methods based on the stress intensity factors also consider the crack propagation in mixed mode, like in the Wood Handbook of the Forest Product Laboratory [35]. It is based on the works of Murphy [31], combining mode I and mode II in mixed mode fracture criterion. This method is similar to the one of the Australian standard [3], which is proposed by Walsh and Leicester [40, 24]. Most methods consider that the wood has a pure brittle behaviour. However, some studies [22, 38] using image correlation measurements, showed the quasi-brittleness of wood [28] in notched beams. The progressive damage is governed by microcracking and crack bridging at notch [7, 28, 30]. Those studies exhibit that the ratio between mode I and mode II of crack extension evolves along the crack path, which questions the reliability of the methods considering only mode I or a constant ratio for mixed mode. This may explain why in some design rules, like the DIN 1052 of 1988 [12], several equations can be proposed, according to the notch geometry, to predict the strength of the beams.

Concerning the reinforced beams, no design rules are present in the Eurocode 5. During the World Conference on Timber Engineering in 2016 (WCTE), some formulations were proposed [11].They are extracted from the DIN 1052 [5], and they are relative to the use of screws as reinforcement. This expression is based on the works performed by Henrici [20], which used the beam theory and the plate theory to estimate the tensile force ($F_{t,90,d}$) supported by the reinforcement [2] and located behind the corner of the notch. This expression was then validated by an experimental campaign carried out by Blaß and Bejtka [6]. The strength of wood is not taken into account, although Coureau [9] demonstrated the interest to consider it.

$$F_{t,90,d} = k_1[3(1-\alpha)^2 - 2(1-\alpha)^3]V_d \tag{2}$$

The Equation 2 requires the determination of the coefficient k_1, depending of the orthotropy and the notch geometry (α , β).

The DIN fixed this coefficient equal to 1.3, which gives a conservative prediction of the load-bearing capacity of reinforced notched beams for $\alpha < 0.8$ and $\beta < 0.2$ [34]. Henrici extended this application field to $\beta < 0.3$, which is recommended by Dietsch [11] in the proposal for the Eurocode 5. However, the approach is limited to small notch size. So, Foliente *et al.* [17], by considering more accurately the stress field at the notch corner, proposed a formula (Equation 3) which can be used for every notch geometry, contrary to the expression of the DIN.

$$F_{t,90} = [3(1-\alpha) - 6(1-\alpha)^2 + 4(1-\alpha)^3]\frac{\beta V_d}{1.12(1-\alpha)} \tag{3}$$

For reinforcements with screws, the mechanical performances of beams are deduced from the ultimate axial load ($R_{ax,d}$), which depends mainly on the anchorage length and the strength of the steel. By neglecting the strength of wood , the resulting bearing capacity is proportional to the number of screws, n (Equation 4).

$$V_d = \frac{n.R_{ax,d}}{1.3[3(1-\alpha)^2 - 2(1-\alpha)^3]} \tag{4}$$

Jockwer [22] evaluated the horizontal force located in the reinforcement due to the shear force, justifying better the conclusions given in the COLORETIM project [8]. Moreover, during experimental campaign, some failures of the beams are due only to the splitting of timber without presenting damage and failure close to the screws. The author confirmed that the crack propagation initiation occurs at the same strength for reinforced and unreinforced beams, which was previously observed by Coureau [9] in the case of beams reinforced with external Plates of Glass Fiber (GFP). Consequently, by only considering the tensile force in the reinforcements ($F_{t,90,d}$), the expression of the DIN 1052 (Equation 4) can not cover the potential failure mechanism produced by the progressive splitting of wood. Moreover, this method was designed only for screw reinforcements. In order to consider this mechanism Coureau [9] expressed the resulting strength of the reinforced beams (V_u) as a combination (Equation 5) of the load bearing capacity of the unreinforced notched beam and an additional strength produced by the reinforcement (V_r^0). This one was governed by the anchorage strength of the glued GFP. During experimental test, failures of elements were activated by the delamination of the glued interface between timber and GFP.

$$V_u = V_u^0 + V_r^0 \tag{5}$$

Few approaches are proposed for reinforced notches beams. The consideration of the interaction between progressive damage and crack extension in wood and the force supported in reinforcements represents a challenge for new design rules. This study proposes a new approach to predict the ultimate load of reinforced and unreinforced wooden notched beams by taking into account the mechanical performance carried out by strength of the wood and by considering its quasi brittleness. The objective is also to supply some useful design methods for reinforced elements presenting failures, elements which are not currently considered by the design approaches.

2. Fracture mechanics

The fracture mechanics was first presented by Griffith [18] which only considered the case of a brittle material. Thus, this approach is not well adapted to the wood, since a non elastic zone appeared ahead to the crack tip [28, 10, 32]. This damaged area is called Fracture Process Zone (FPZ), and presents micro-cracking and crack bridging [4, 29, 32]. The quasi-brittleness of wood has an effect on the resulting performance, since the energy released by the wooden element is used for damage and crack extension. This type of material can be considered by two different methods, a non-linear one, which is based on the cohesive law (cohesive crack model) [13, 33, 29, 30, 39], and a linear one as part of the equivalent Linear Elastic Fracture Mechanics ($_{\text{EQ}}$LEFM), which considers a Resistance to crack growth-curve (called, R-curve) [4, 41, 28, 26, 10].

The cohesive crack models can be implemented in a Finite Element Model (FEM) for crack propagation in pure mode or mixed mode. However, these models require substantial computing resources. Moreover, the properties governing the softening behaviour of the material are not easy to characterise [32], especially the ultimate separation of wood in mode I and II. The $_{\text{EQ}}$LEFM requires less calculation resources, since the crack propagation is computed by considering pure elastic material. The damage and crack extension are determined by energetic balance. This method allows to characterise a crack propagation in mixed mode by using the Resistance-curves (R-curves) [23] in mode I and mode II, which are regarded as mechanical properties of wood.

3. Model for the splitting of wood

3.1. Equivalent Linear Elastic Fracture Mechanic ($_{\text{EQ}}$LEFM)

The $_{\text{EQ}}$LEFM consider a crack length (Δa) to describe the fracture mechanisms in a quasi-brittle material. Δa is determined by considering that the compliance variation of the element (λ) -only due to the damaging and the crack propagation- is equivalent to the one ($\lambda_{elastic}$) due to the extension of a single crack in a purely elastic material with the same geometry. Then, the energy release rate (G) can be determined according to the crack length (Δa) (Eq. 6) [28].

$$G(\Delta a) = \frac{P^2}{2b}\frac{d\,\lambda(\Delta a)}{d\,\Delta a} \tag{6}$$

The crack propagates when the energy release rate reaches a critical value depending on the material resistance. The difference between brittle and quasi-brittle behaviour can be observed on a $G_R(\Delta a)$ diagram (Figure 2). In the

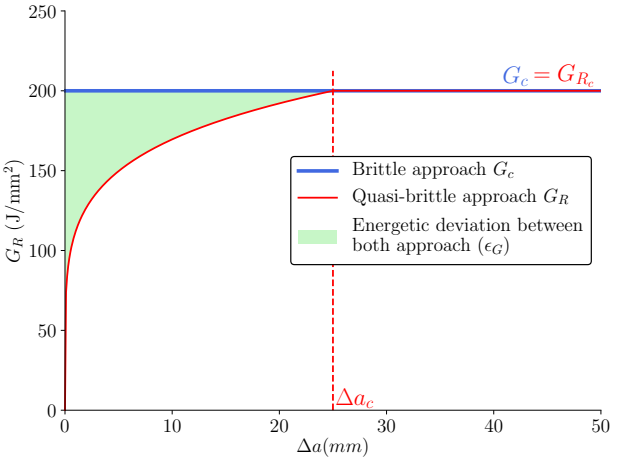

Figure 2: $G_R(\Delta a)$ diagram for brittle and quasi-brittle material

case of a brittle material, the crack propagation starts when the critical energy release rate (G_c) is reached, whatever the crack length is, with G_c as a material property. On another hand, for quasi-brittle material, the crack propagation in the wooden element depends on an R-curve, which is a function of the critical energy release rate versus (Δa) with two phases. The first regime (Figure 2), corresponding to an increase of the energy, governs the damage development, whereas the plateau corresponds to the auto-similar crack propagation, as for a brittle material.

This highlights how considering the wood as a pure brittle material can lead to an overestimation of the load-bearing capacity of the beam. Indeed, if the failure of the element occurs before the plateau is reached (for a crack length inferior to Δa_c), the brittle approach will overestimate the energy consumed by the crack propagation and the resulting strength.

3.2. Model principle

As mentioned previously, the crack propagation in notched beams is produced by mixed mode, in order to supply a reliable prediction, the quasi-brittle behaviour of wood must be considered in mode I and mode II. The model proposed by Lartigau *et al.* [23] for structural gluing may be adapted to the wooden notched beam configuration. It can supply a prediction of the load/displacement curve of a structural element by considering its critical R-curve ($G_R^*(\Delta a)$). This load/displacement curve is determined by considering for each crack length Δa a critical load P_c and a critical displacement δ_c, obtained by using equations 7 and 8. In this method, the compliance variation $\lambda(\Delta a)$ is computed for 1 N load, as part of linear elasticity, by simulating the propagation of a crack in the considered structure using a finite element model.

$$P_c(\Delta a) = \sqrt{\frac{2bG_R^*(\Delta a)}{\lambda'(\Delta a)}} \tag{7}$$

$$\delta_c(\Delta a) = \lambda(\Delta a).P_c(\Delta a) \tag{8}$$

The determination of $G_R^*(\Delta a)$ is defined by using mixed mode criterion (Eq. 9) taking into account the wood R-curves relative to mode I and II ($G_{R_I}(\Delta a)$ and $G_{R_{II}}(\Delta a)$). It governs the potential damage and crack extension, producing progressive or sudden splitting mechanism, in the considered element.

$$\left(\frac{G_I(\Delta a)}{G_{R_I}(\Delta a)}\right)^p + \left(\frac{G_{II}(\Delta a)}{G_{R_{II}}(\Delta a)}\right)^q = 1 \tag{9}$$

This criterion can have different forms, linear (p =1, q=1), quadratic (p=2, q=2) or semi-quadratic (p=1,q=2 or p=2, q=1). In the case of notched beams the mixed mode ratio evolves from mode I to mode II, even more in the case of reinforced beams. So in order to simplifies the expression and in accordance with the phenomenon observed, the linear criterion was used for this study which leads to the following expression of $G_R^*(\Delta a)$ (Eq. 10).

$$G_R^*(\Delta a) = \left(\frac{G_I(\Delta a)/G_{I+II}(\Delta a)}{G_{R_I}(\Delta a)} + \frac{G_{II}(\Delta a)/G_{I+II}(\Delta a)}{G_{R_{II}}(\Delta a)} \right)^{-1} \tag{10}$$

In this expression $G_{I+II}(\Delta a)$ is the global energy release rate, in the meaning of the $_{\text{EQ}}$LEFM, calculated, for each crack length Δa as the sum of $G_I(\Delta a)$ and $G_{II}(\Delta a)$ the energy release rate for both pure modes I and II ($G_{I+II}(\Delta a) = G_I(\Delta a) + G_{II}(\Delta a)$).

The expression of the R-curves in pure mode is a two part function of three parameters, with a power law following by a plateau value [27, 10] (Eq. 11). The critical energy release rate $G_{R_{c_i}}$, the critical crack length Δa_{c_i} and the law factor β_i must be determined on the considered wood species for each pure mode i (Figure 2).

$$G_{R_i}(\Delta a) = \begin{cases} G_{Rc_i} \left[\frac{\Delta a}{\Delta a_{c_i}} \right]^{\beta_i} & if \quad \Delta a < \Delta a_{c_i} \\ G_{Rc_i} & if \quad \Delta a \geq \Delta a_{c_i} \end{cases} \tag{11}$$

This approach comes with some hypotheses. At first, the crack path is supposed to be known, which is in accordance with the splitting failure. The propagation occurs along the wood grain and the crack initiation is located at the singularity (stress concentration area). Moreover, this model is performed by assuming plane strain, which implies that the crack tip is perpendicular to the span of the beam. For a sack of simplicity, we consider here that the splitting of wood is produced only by shear stress along the grain and tensile stress perpendicular to the grain direction. Mode III of crack propagation is neglected at first. During experimental campaign, some measurements were performed to check this hypothesis.

3.3. Notched beam application

In the case of unreinforced notched beams, the approach aims at evaluating the critical energy curve ($G_R^*(\Delta a)$) of the structural element in function of the notch geometry(α and β) and the mechanical properties of timber (elastic moduli and R-curves). In the case of reinforced beams, the state of the art shows that several failure mechanisms may occur. However, by taking into account the splitting of wood, it is possible to improve and to complete the existing predictions.

As a first approximation, the effect of the reinforcement can be implemented in the FEM by considering kinematically the perfect connection between two opposite nodes at the lips of the crack on the reinforcement axis (Figures 3 and 4). Consequently, there is no relative displacement between the opposite nodes, so the vertical and horizontal stiffness (K_v and K_h) of the reinforcement are considered infinite. It is possible to obtain the progressive load transfer between wooden substrate and screws. The closure located on the crack path suggests that no damage occurs in the reinforcement and that the crack can propagate ahead and behind it. The potential complexity of the damage zone around the reinforcement locality is regarded only by assuming the compliance variation of the specimen.

In reinforced cases, the proposed model leads to a deviation of the compliance evolution (λ) according to the crack length (Δa) in comparison with an unreinforced beam (Figure 5). This deviation produces the bifurcation of the propagation modes from the mode I to the mode II (Figure 6). Indeed, the local closure on the crack path produces a new repartition between the crack propagation mechanisms at the tip of the crack.

Consequently, the splitting of wood is governed by a new mixed mode ratio which favours the mode II rather than the mode I. Thus, the resulting strength of the component is modified, without considering any damage in the reinforcement (Figure 7). This increase of $G_R^*(\Delta a)$ leads to an increase of the load-bearing capacity of the beam (P_u). The rise of the mechanical performances is mainly due to the difference of energy necessary to propagate a crack in mode II rather than mode I (Figure 8). Indeed, the fracture energy in mode II is 3 or 4 times higher than the mode I, depending on the wood species [2, 37]. As part of linear fracture mechanics (Equation 7), this difference of energy leads to an improvement of the load by a factor 2, in comparison with the strength of unreinforced element.

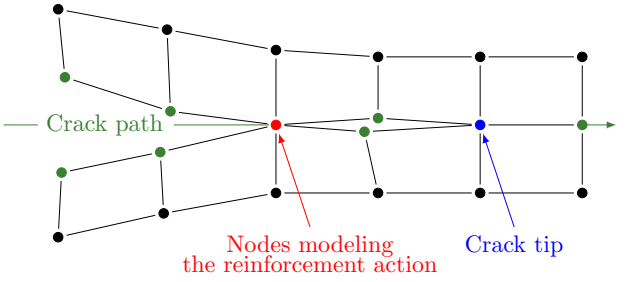

Figure 3: Boundary conditions imposed on the crack path to model the reinforcement system

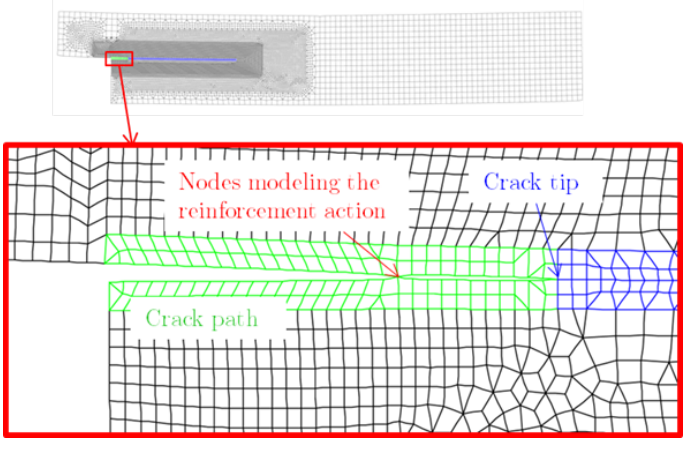

Figure 4: Example of a mesh deformation observed at the crack tip locality with an amplification of 1.10^3

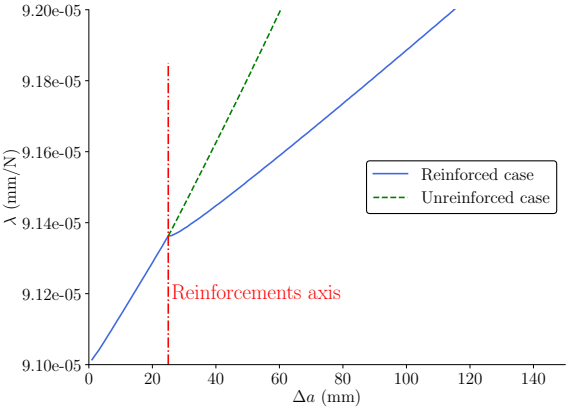

Figure 5: Comparison between the evolution of the compliance for a reinforced and an unreinforced beam of the same geometry

Consequently, the recommendations given in literature and standard are more justified by this observation, since they limit the strength of reinforced beams with a similar ratio [11]. Moreover, figure 6 illustrates that crack propagates between the corner of the notch and the reinforcement axis with the same ratio of mode I and II than the unreinforced beam (curves are superimposed). This induces that the crack initiation occurs for the same load level in both cases, which was experimentally observed by Coureau [9] and Jockwer [22].

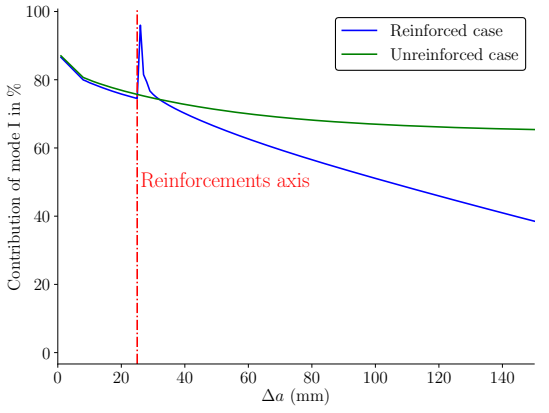

Figure 6: Evolution of the contribution in mode I in the global crack propagation, according to Δa, for the reinforced and the unreinforced case

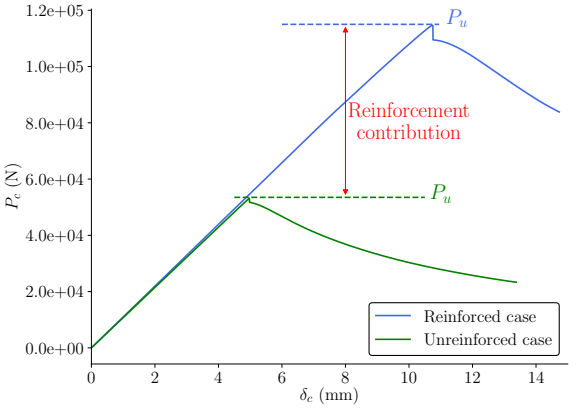

Figure 7: Comparison between the predictive load/displacement curves of a reinforced and an unreinforced beam of the same geometry

4. Validation by experiments

The first aim of the experiments carried out in this study is to validate the hypotheses made by the proposed model and in a second time to compare the relevance of the prediction of the model to the one of the current design rules proposed for notched beams with and without reinforcement. In this part of the article only the validity of the hypotheses are discuss and the comparison with the current design rules will be made in a second part. Two experimental campaigns were carried out on GL24h (Spruce) by performing three points bending test (Figure 1) in controlled displacement (2mm/min) with a force cell capacity of 250 kN. The first one was performed on small beams of 168X89 mm^2 and 990 mm span. The parameters of the notch were $\alpha = 0.5$ and $\beta = 0.6$. Two different reinforcement configurations using SFS WT-T6.5X160 screws were tested. One with a single screw and another one with three screws located along the width of the beam (placed at 20 mm behind the corner of the notch). The second experimental campaign was carried out on larger beams of 495X115 mm^2 and 3500 mm span. Two different notch geometry are chosen for the unreinforced case ($\alpha = 0.66$ and $\alpha = 0.8$) for a given β equal to 0.6. For reinforced beams, two configurations were tested for a given notch size $\alpha = 0.66$ and $\beta = 0.6$: two screws and three screws along the width were placed in the structural element. SFS WR-T-9X350 reinforcements are used for this. The location of the reinforcement follows recommendations given by Dietsch [11], with an axis at a distance of 25 mm behind the notch corner. The ultimate shear strength of the beams tested are given by tables 1,2 and 3.

During test, the displacement under the load axis was measured, by avoiding the crushing at supports, in order to measure accurately the mechanical energy released by the damage and the potential crack extension in the component

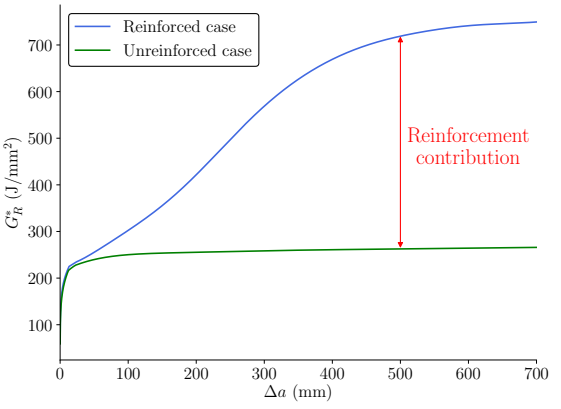

Figure 8: Comparison between the critical R-curve ($G_R^*(\Delta a)$) of a reinforced and an unreinforced beam

Table 1
Tests result for the first experimental campaign

Configuration ($\alpha = 0.5$)	Unreinforced	3 screws
V_u (N)	9500	24120
Standard deviation (N)	2050	1780
CoV (%)	22%	7%
Number of test	5	6

Table 2
Tests result for the second experimental campaign

Configuration ($\alpha = 0.66$)	Unreinforced	2 screws	3 screws
V_u (N)	39600	84500	77800
Standard deviation (N)	5260	12360	11160
CoV (%)	13%	15%	14%
Number of test	6	3	3

Table 3
Tests result for the second experimental campaign (unreinforced configurations)

Configuration	$\alpha = 0.66$	$\alpha = 0.8$
V_u (N)	39600	58300
Standard deviation (N)	5260	5770
CoV (%)	13%	10%
Number of test	6	4

(Figure 9(a)). An image correlation system was also used to measure the strains fields around the notch (Figure 9(b)).

4.1. Reinforced case

The image correlation measurement shows that the out-of-plane displacements are negligible. These observations are in accordance with the hypothesis taken in the proposed model. The failure of the beam is due to a sudden instability of the crack produced by splitting, which generates a significant loss of stiffness. Moreover, as shown by the model, the crack propagation initiates at the same load level for reinforced notched beams and unreinforced ones. The reinforcement has no effect for crack length located between its axis. The failure of the beams is only due to the splitting of wood and there is no visible opening on the crack path close to the screws. So, the reinforcement integrity remains

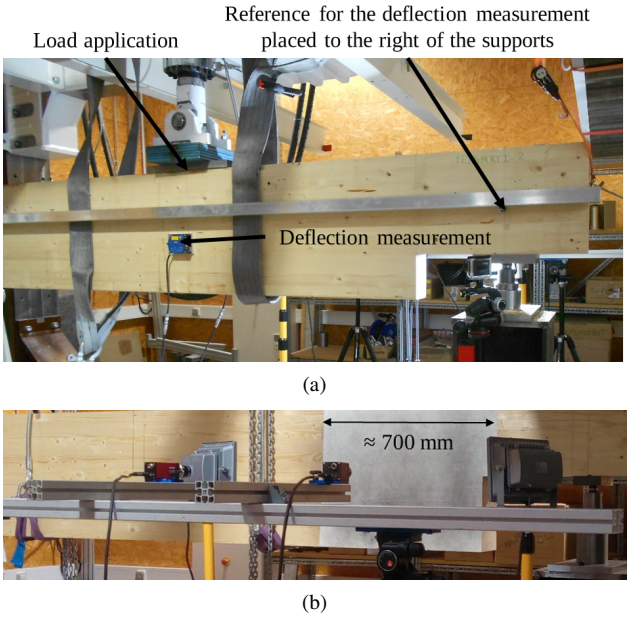

Figure 9: Experimental device (a) with the stereo-vision measurement system (b)

intact and no failure nor excessive displacements are observed. For this configuration, timber is the weakness link but still contributes to the mechanical performances of the reinforced beams. The average gain obtained experimentally is close to 100% (Tables 1 and 2).

Screws prevent the opening of the crack, as it can be observed with the image correlation measurement around the notch (Figure 10). Strains due to the tensile stress perpendicular to the grain (ϵ_{yy}) is stopped forward the reinforcement axis, whereas strains due to shear (ϵ_{xy}) is not fully prevented.

However, for reinforcement composed of only one screw the crack may propagate in the vicinity of it. In this case, a macro crack appears on each side of the beam, and the strains produced by the mode II seems to be less important (Figure 11) than for the configuration with 3 screws (Figure 10). This is due to a non-fully block of the local crack opening which induces a more active mode I. As a consequence, the mode I requiring less energy to create a crack extension in the macro splitting mechanism than the mode II, the resulting strength of the beam is lower than the one with 3 screws.

In the case of reinforced beams with a crack opening perfectly locked on the reinforcement axis, along the width of the beam. The proposed model indicates that compared to unreinforced beams, the mixed mode crack propagation ratio evolves from mode I to mode II (Figure 6). This was observed experimentally by using image correlation (Figure 10). For a given notch, the decrease of mode I along the crack path is close to 20% (Figure 6). Experiments found in the literature illustrate that the mechanical performance of reinforced elements depends on both reinforcement and wood strength [22]. Consequently, several failure mechanisms should be predicted and the splitting of wood in the reinforced notched beams should be part of it as a potential failure scenario.

The model for the splitting of wood proposed in this article uses the R-curves and so takes into account the quasi-brittle behaviour of wood. This is a new tool to appreciate the mechanical performance of the reinforced solutions. It describes better the mechanisms acting on the improvement of the resulting strength of beams, which is mainly due to a new distribution between mode I and II on the crack path. The bridging produced by the screws reduces the part of mode I, which improves the mechanical performance. When splitting governs the failure of the beam, the number of screws is not directly proportional to the load bearing capacity. This observation is illustrated in the second experimental campaign, where the mean ultimate load remains the same for a two or three screws reinforcement system (Table 2).

In this case, the improvement of the strength between reinforced and unreinforced elements is governed mainly by the increase of the energy release rate produced by the local crack closure. So, the increase of the ultimate load

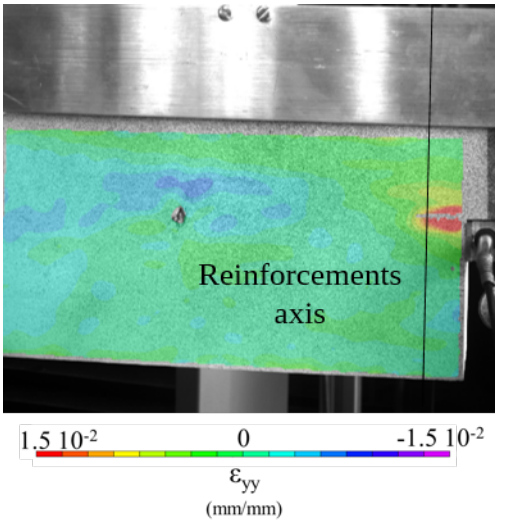

(a)

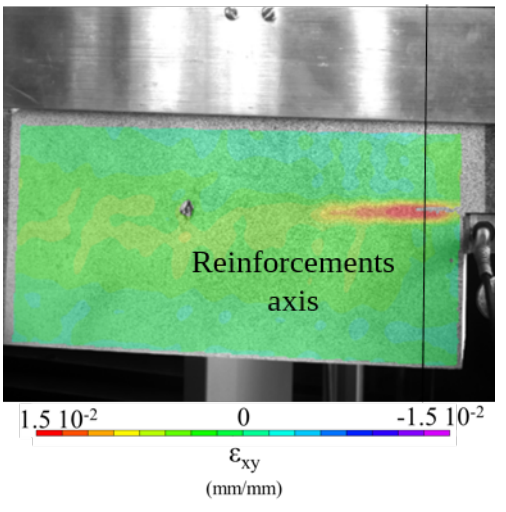

(b)

Figure 10: ϵ_{yy} (a) and ϵ_{xy} (b) strains fields for a beam reinforced with three screws, one second before its failure

depends on the ratio between mode I and mode II : the higher the mode II is, the higher the load bearing of the beam is. Consequently, the maximum increase of the resulting strength is limited by the R-Curve of wood in mode II according to the geometry. This phenomenon is taken into account in the model by equation 10.

4.2. Unreinforced case

The unreinforced beams present a progressive decrease of the stiffness, which is observed by a non-linear regime at the end of the load/displacement curves. The damage is initiated at the corner of the notch. It is significant and influences the ultimate load of the notched beams (Figure 12). Consequently, the use of R-curve for the prediction seems to be a really appropriated characteristic to evaluate the mechanical performance of those elements.

By considering mixed mode crack propagation using R-curves the proposed model helps to predict the load-bearing capacity of structural element, when splitting contribute to the strength. For notched beams the contribution of mode I and mode II in splitting is relative to the shape and size of the notch (α and β). For important α, the mode II is more active and requires more energy than the mode I to damage and propagate a crack in wood. This leads to an increase of the strength of the beam governed by the function (G_R^*) and the R-curves (wood fracture properties). Experimental

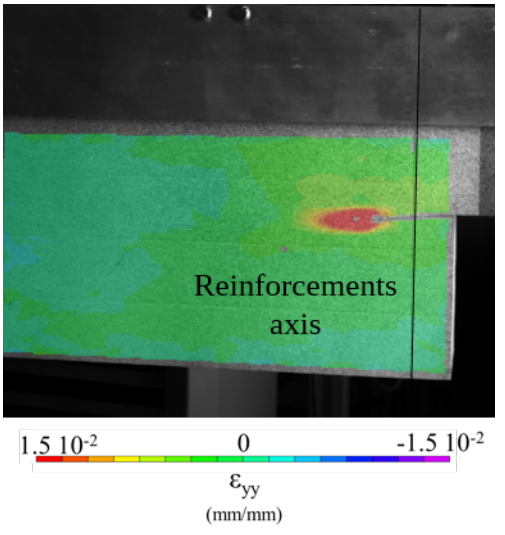

(a)

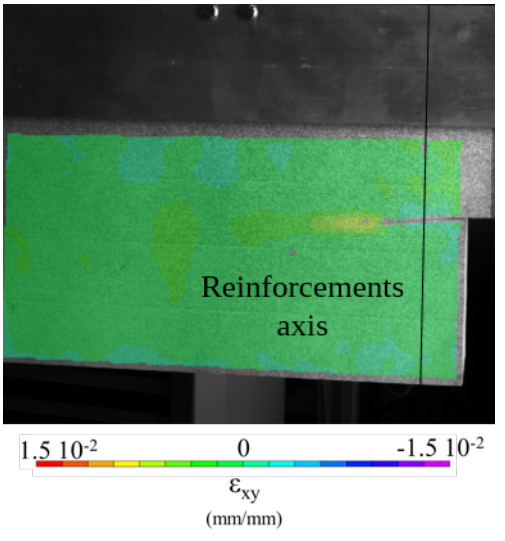

(b)

Figure 11: ϵ_{yy} (a) and ϵ_{xy} (b) strains fields for a beam reinforced with one screw, one second before its failure

results confirm this tendency (Table 3). When β increases for a given notch height, mode I rises and performance declines. Consequently, the splitting of wood appears in all configurations but the mixed mode contribution (given by equation 9) leads to different strength levels according to the geometry of notched beams. The proposed method takes into account these variations.

To conclude, the experimental observations made are in accordance with the proposed model hypotheses and principle. So, the corresponding predictions can be compared to those obtained with the current design rules and the experimental data. In order to appreciate the different approaches, the input material properties implemented in the models are presented in the tables 4, 5 and 6.

5. Comparison with current design rules

In order to compare the relevance of two predictive methods, the comparison must be done for every test. Indeed the comparison of the mean values does not show if the prediction is always conservative. This can lead to an over-

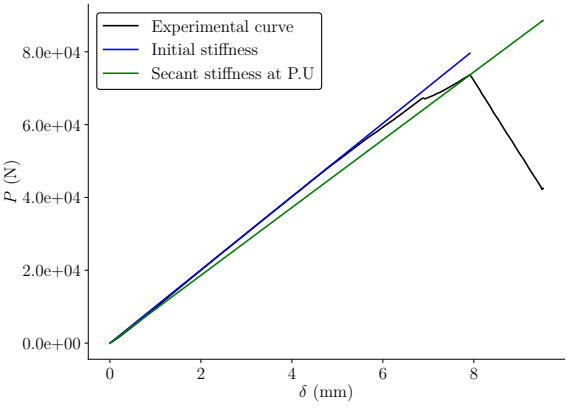

Figure 12: Example of an experimental curve with the initial stiffness (elastic behaviour) and the secant stiffness at ultimate load of an unreinforced beam

Table 4
Elastic properties used as input parameters of the models [37]

E_L	E_T	E_R	G_{LR}	ν_{LT}	ν_{RL}	ν_{RT}
11430	560	905	780	0.47	0.37	0.44

Table 5
Fracture properties used as input parameters of the models [37]

G_{Rc_I}	Δa_{c_I}	β_I	$G_{Rc_{II}}$	$\Delta a_{c_{II}}$	β_I
190	12	0.14	780	22	0.54

Table 6
Distance between the reinforcement system axis and the notch extremity ($a_{3,c}$)

First campaign	Second campaign
20 mm	25 mm

estimation of the load-bearing capacity for some element and can question the safety of the method. So, in order to compare the relevance of the proposed method to the one of the current design rules, a relevance ratio was determined for each test (Eq. 12).

$$R_{relevance} = \frac{V_{exp}}{V_{approach}} \tag{12}$$

In this expression V_{exp} is the experimental shear force, and $V_{approach}$ the predictive shear force given by the proposed model, and by the Gustafsson's formula (Equation 1) for unreinforced beams or the DIN 1052 formula (Equation 4) for reinforced beams.

5.1. Unreinforced case

In order to make a comparison, the elastic properties implemented in the Gustafsson's design rule are similar to the ones used in the model (Table 4). The critical energy release rate in mode I ($G_{c,I}$) is taken equal to the plateau value of the R-curve in mode I ($G_{R_{c_I}}$) (Table 5). The cumulative frequency distribution of the relevance ratio are presented in figure 13. It shows that the proposed model is globally more conservative than the Gustafsson's approach and that two predictions made by the Gustafsson's approach are non-conservative against only one for the proposed model.

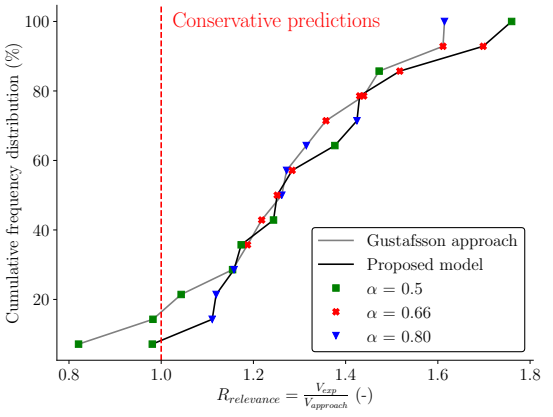

Figure 13: Cumulative frequency distribution of the relevance ratio ($R_{relevance}$) for the proposed model and the Gustafsson's approach

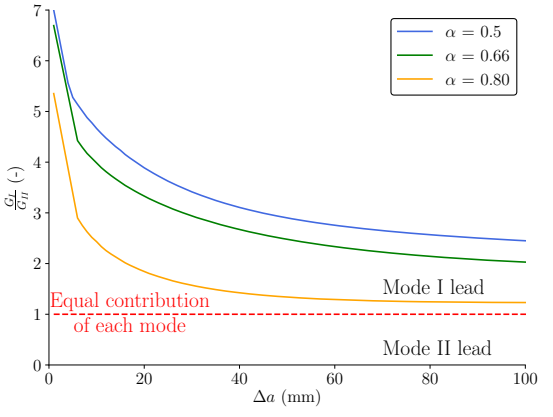

Figure 14: Evolution of the mixed mode ratio for different α parameter (results obtained from the numerical model)

However, simulations made for different values of α parameter show that the mode I and II distribution is different according to the notch geometry, with a greater contribution of mode II for higher values of α(Figure 14). So, for example if α is equal to 0.8, the Gustafsson's approach, which only consider the mode I, will be more conservative (Figure 15). But, this approach is not well adapted for splitting where the mode II is predominant. On the contrary, the equation 10 takes into account, by using $G_I(\Delta a)$ and $G_{II}(\Delta a)$, the influence of the notch geometry (α and β parameters) on the mixed mode ratio.

Moreover, Smith and Springer [36] explained that the evolution of the stiffness is crucial to predict correctly the ultimate load using the fracture mechanics, and that its current determination in the Eurocode 5 design rules may represent a bias in the method. So, to prevent such bias, the mode II and its corresponding R-curve must be considered in the splitting of wood mechanisms. Indeed, although its contribution in structural component geometry may be low, by being much more energetic, the mode II concentrates a non-negligible part of the global energy released by the element, and so limits the crack extension in mode I. By considering the mode II in equation 10, the proposed model provides a useful tool for prediction, nevertheless the R-curves of the material are required.

5.2. Reinforced case

The FE-model is compared to the approach of the DIN 1052 (Equation 4), which only considers the strength of the reinforcement (screws), which characteristics are presented in table 7.

The cumulative frequency distribution of the relevance ratio ($R_{relevance}$) relative to both approaches (Figure 16) shows that the expression of the DIN 1052 overestimates the strength of the beams reinforced by three screws of

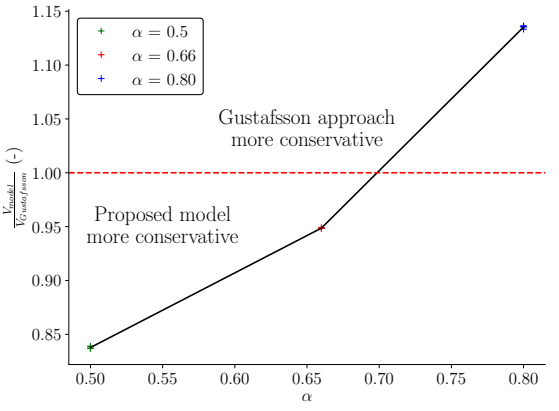

Figure 15: Comparison between the prediction made by the proposed model and the Gustafsson's approach

Table 7
Characteristics of the reinforcement

Paramaters	WT-T-6.5X160	WR-T-9X350
External diameter (mm)	6.5	9
Length (mm)	160	350
$f_{ax,k}(N/mm^2)$	12.9	12.8
$R_{t,u,k}(kN)$	14.4	35.9

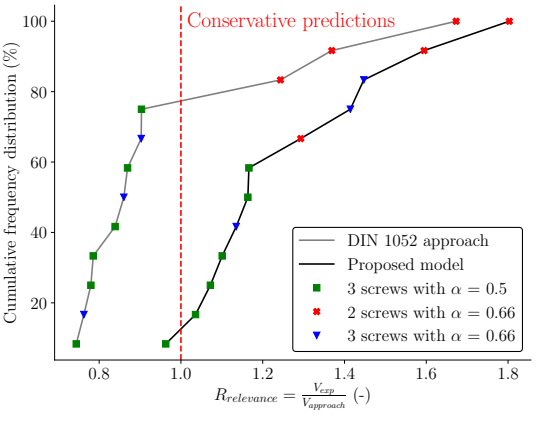

Figure 16: Cumulative frequency of the relevance ratio ($R_{relevance}$) for the proposed model and the DIN 1052 approach

about 20%. But for the two screws reinforcements, the predictions are conservative. On another hand, the proposed model provides conservative predictions for almost every test. Moreover, the two and three screws reinforcements are distributed in a more homogeneous way. This difference is due to the failure scenario considered in each approach. Indeed, the DIN 1052 only considers the failure of the reinforcement system, when the proposed model only considers the failure caused by a crack propagation in the wood, which was the only scenario experimentally observed.

The values of V_{exp} and $V_{approache}$ are provided in tables 8 and 9 to be more explicit. For the proposed model and the Gustafsson's formula, the elastic properties are corrected by a coefficient calculated on the initial stiffness for each specimen. This correction method was proposed by Morel *et al.* [29].

So, in conclusion, the DIN 1052 can lead to an overestimation of the load-bearing capacity of reinforced notched beams, if the crack extension in wood is not considered. On another hand, the proposed model provides a useful tool, which could be added to the current Eurocode 5 proposal [11] in order to give a better prediction of the potential failure

Table 8
Experimental and predictive shear strengths (in kN) of unreinforced beams

Configuration	V_{Gus} (CoV)	V_{model} (CoV)	V_{exp} (CoV)
$\alpha = 0.5$	8.7 (2%)	7.3 (8%)	9.5 (22%)
$\alpha = 0.66$	28.2 (2%)	26.8 (2%)	39.5 (13%)
$\alpha = 0.8$	42.8 (2%)	48.6 (2%)	48.6 (2%)

Table 9
Experimental and predictive shear strengths (in kN) of reinforced beams

Configuration	V_{DIN} (CoV)	V_{model} (CoV)	V_{exp} (CoV)
$\alpha = 0.5$ (3 screws)	29.4 (0%)	22.2 (2%)	24.1 (7%)
$\alpha = 0.66$ (2 screws)	59.0 (0%)	54.0 (6%)	84.5 (13%)
$\alpha = 0.66$ (3 screws)	88.6 (0%)	56.2 (5%)	74.8 (14%)

mechanism.

6. Conclusion

The splitting of reinforced and unreinforced structural timber beam is investigated in this study. Numerical computations are proposed to evaluate the strength of beams, in which crack may propagate in mode I and mode II. In order to take into account the quasi-brittleness of wood, R-curves are implemented in a mixed mode criterion, which governs the macro-splitting of the element. Experiments performed are in good agreement with the prediction for reinforced and unreinforced cases. So, the assessment of R-Curves allows to understand the contribution of mode I and mode II on the splitting of wood mechanisms and the corresponding mechanical performances.To summarize, if the mode II is preponderant, the load-bearing capacity of the beam is higher. Moreover, the study exhibits that a change in the boundary conditions on a potential crack path, by the addition of reinforcement for example, modifies the mixed mode distribution at the crack tip.

The numerical computations exhibit a good accordance with experiments and a better prediction than the one extracted from literature. Finally, it is possible to predict splitting failure scenarios which are not covered by Eurocode 5 or DIN 1052, in the case of reinforced beams. It supplies also, better prediction of the ultimate load bearing capacity which are characterised by R-curve in mode I and II.

To conclude, the proposed approach gives a new tool to evaluate the load-bearing capacity of structural elements in which splitting may occur. Moreover, by using the equivalent linear elastic fracture mechanics, the variability of wood can be considered in the compliance (elastic properties) and the R-curves (fracture properties). Consequently, this approach can be used to calibrate some predictions for the reliability of structural components.

7. Acknowledgments

The authors wants to thank the Reasearch National Agency of France (ANR) for its participation across the Xyloplate project (ANR-10-EQPX-16), the CODIFAB for its financial supports and the SFSintec company for its generous donations of screws.

References

[1] Aicher, S., Gustafsson, P.J., Haller, P., Petersson, H., 2002. Fracture mechanics models for strength analysis of timber beams with a hole or a notch - A report of RILEM TC-133. Technical Report. Lund University. Lundo and Espoo.

[2] Anh, P.N., Stéphane, M., Myriam, C., Jean-Luc, C., 2014. R-curve on Fracture Criteria for Mixed-mode in Crack Propagation in Quasi-brittle Material: Application for Wood. Procedia Materials Science 3, 973–978. URL: http://www.sciencedirect.com/science/article/pii/S221181281400159X, doi:10.1016/j.mspro.2014.06.158.

[3] AS 1720.1-1997, 1997. Timber structures - design methods. Timber Structures: Design Methods .

[4] Bazant, Z.P., Planas, J., 1997. Fracture and Size Effect in Concrete and Other Quasibrittle Materials. CRC Press.

[5] Blaß, H.J., 2004. Erläuterungen zu DIN 1052: 2004-08: Entwurf, Berechnung und Bemessung von Holzbauwerken. DGfH.

[6] Blaß, H.J., Bejtka, I., 2004. Reinforcements perpendicular to the grain using self-tapping screws, in: The 8th world conference on timber engineering, Lahti, Finland. URL: http://holz.vaka.kit.edu/public/37.pdf.

[7] Boström, L., 1994. The stress-displacement relation of wood perpendicular to the grain. Wood science and technology 28, 309–317.

[8] COLORETIM, 2001. European project COLORETIM final report. Technical Report. L.R.B.B.

[9] Coureau, J.L., 2002. Renforcement local d'éléments de structures bois par des matériaux composites. Ph.D. thesis. Bordeaux 1. URL: http://www.theses.fr/2002BOR12508.

[10] Coureau, J.L., Morel, S., Dourado, N., 2013. Cohesive zone model and quasibrittle failure of wood: A new light on the adapted specimen geometries for fracture tests. Engineering Fracture Mechanics 109, 328–340. URL: http://www.sciencedirect.com/science/article/pii/S0013794413000763, doi:10.1016/j.engfracmech.2013.02.025.

[11] Dietsch, P., 2016. Reinforcement of timber structures - a new section for Eurocode 5, Vienna. p. 10.

[12] DIN 1052, 1988. Holzbauwerke .

[13] Elices, M., Guinea, G., Gomez, J., Planas, J., 2002. The cohesive zone model: advantages, limitations and challenges. Engineering fracture mechanics 69, 137–163.

[14] EN 14080, C., 2013. Timber structures. glued laminated timber and glued solid timber. requirements .

[15] EN 338, 2009. Structural timber - strength classes .

[16] Eurocode 5, 2004. Eurocode 5 : Design of timber structures - Part 1-1: General - Common rules and rules for buildings .

[17] Foliente, G.C., McLain, T.E., 1992. Design of notched wood beams. Journal of Structural Engineering 118, 2407–2420.

[18] Griffith, A.A., 1921. VI. The phenomena of rupture and flow in solids. Phil. Trans. R. Soc. Lond. A 221, 163–198. doi:10.1098/rsta.1921.0006.

[19] Gustafsson, P.J., 1988. A study of strength of notched beams, Parksville, Canada.

[20] Henrici, D., 1984. Beitrag zur Spannungsermittlung in ausgeklinkten Biegeträgern aus Holz. Ph.D. thesis. Technische Universität München.

[21] Irwin, G.R., 1958. Fracture. Handbuch der Physik , 551.

[22] Jockwer, R., 2014. Structural behaviour of glued laminated timber beams with unreinforced and reinforced notches. Ph.D. thesis. ETH ZURICH. Zurich.

[23] Lartigau, J., Coureau, J.L., Morel, S., Galimard, P., Maurin, E., 2015. Mixed mode fracture of glued-in rods in timber structures. International Journal of Fracture 192, 71–86.

[24] Leicester, R., Walsh, P.F., 1983. Numerical analysis for notches of arbitrary notch angle, in: Fracture Mechanics Technology Applied to Material Evaluation and Structure Design. Springer, pp. 161–170.

[25] Linville, J.D., et al., 2012. Timber construction manual. John Wiley & Sons.

[26] Morel, S., 2007. R-curve and size effect in quasibrittle fractures: Case of notched structures. International Journal of Solids and Structures 44, 4272–4290. URL: http://www.sciencedirect.com/science/article/pii/S0020768306004835, doi:10.1016/j.ijsolstr.2006.11.014.

[27] Morel, S., Dourado, N., 2011. Size effect in quasibrittle failure: Analytical model and numerical simulations using cohesive zone model. International Journal of Solids and Structures 48, 1403–1412.

[28] Morel, S., Dourado, N., Valentin, G., 2005. Wood: a quasibrittle material R-curve behavior and peak load evaluation. International Journal of Fracture 131, 385–400. URL: http://link.springer.com/10.1007/s10704-004-7513-0, doi:10.1007/s10704-004-7513-0.

[29] Morel, S., Lespine, C., Coureau, J.L., Planas, J., Dourado, N., 2010. Bilinear softening parameters and equivalent LEFM R-curve in quasibrittle failure. International Journal of Solids and Structures 47, 837–850. URL: http://www.sciencedirect.com/science/article/pii/S002076830900465X, doi:10.1016/j.ijsolstr.2009.11.022.

[30] de Moura, M.F.S.F., Dourado, N., Morais, J., 2010. Crack equivalent based method applied to wood fracture characterization using the single edge notched-three point bending test. Engineering Fracture Mechanics 77, 510–520. URL: http://www.sciencedirect.com/science/article/pii/S0013794409003245, doi:10.1016/j.engfracmech.2009.10.008.

[31] Murphy, J.F., 1979. Using fracture mechanics to predict failure in notched wood beams. Reprints-United States, Forest Service .

[32] Phan, N.A., 2016. Simulation of time-dependent crack propagation in a quasi-brittle material under relative humidity variations based on cohesive zone approach: application to wood. Ph.D. thesis. Bordeaux. URL: http://www.theses.fr/2016BORD0008.

[33] Planas, J., Elices, M., Guinea, G., Gómez, F., Cendón, D., Arbilla, I., 2003. Generalizations and specializations of cohesive crack models. Engineering fracture mechanics 70, 1759–1776.

[34] Robert Jockwer, A.F., 2013. Enhanced design approach for reinforced notched beams .

[35] Ross, R.J., et al., 2010. Wood handbook: Wood as an engineering material. volume 190.

[36] Smith, I., Springer, G., 1993. Consideration of Gustafsson's proposed Eurocode 5 failure criterion for notched timber beams. Can. J. Civ. Eng. 20, 1030–1036. URL: http://www.nrcresearchpress.com/doi/abs/10.1139/l93-133, doi:10.1139/l93-133.

[37] Sorin, E., 2018. Fissuration en modes mixtes dans le bois: diagnostic et évaluation des méthodes de renforcement local. Ph.D. thesis. Université de Bordeaux.

[38] Toussaint, E., Fournely, E., Moutou Pitti, R., Grédiac, M., 2016. Studying the mechanical behavior of notched wood beams using full-field measurements. Engineering Structures 113, 277–286. URL: http://linkinghub.elsevier.com/retrieve/pii/S0141029616000766, doi:10.1016/j.engstruct.2016.01.052.

[39] Tran, D., Oudjene, M., et al., 2018. Experimental and numerical analysis of the unreinforced and reinforced notched timber beam by a screw. Vietnam Journal of Science, Technology and Engineering 60, 26–32.

[40] Walsh, P., Leicester, R., Ryan, A., 1973. strength of glued lap joints in timber. Forest products journal .

[41] Yoshihara, H., 2004. Mode II R-curve of wood measured by 4-ENF test. Engineering Fracture Mechanics 71, 2065–2077. URL: http://www.sciencedirect.com/science/article/pii/S0013794403002790, doi:10.1016/j.engfracmech.2003.09.001.